INSTITUTE OF PLASMA PHYSICS

NAGOYA UNIVERSITY

Generation of Astron-Spherator Configuration

Kazumichi NARIHARA, Mitsuru HASEGAWA
Yukihiro TOMITA, Tetsuya TSUZUKI
Kuninori SATO and Akihiro MOHRI

(Received - Dec.27, 1982)

IPPJ-621 Jan. 1983

RESEARCH REPORT

NAGOYA, JAPAN

Generation of Astron-Spherator Configuration

Kazumichi NARIHARA, Mitsuru HASEGAWA
Yukihiro TOMITA, Tetsuya TSUZUKI
Kuninori SATO and Akihiro MOHRI

(Received - Dec.27, 1982)

IPPJ-621 Jan. 1983

Further communication about this report is to be sent to the Research Information Center, Institute of Plasma Physics, Nagoya University, Nagoya 464, Japan.

Generation of Astron-Spherator Configuration

(°°°°°°° first issue .....)

Kazumichi NARIHARA, Mitsuru HASEGAWA, Yukihiro TOMITA,
Tetsuya TSUZUKI, Kuninori SATO and Akihiro MOHRI

Institute of Plasma Physics, Nagoya University
Nagoya, 464

Synopsis

It was experimentally demonstrated that Astron-Spherator configuration is formed by injecting a pulsed relativistic electron beam in a toroidal device SPAC-VI with external toroidal and vertical magnetic fields. A plasma is confined in the extended magnetic region produced by a slender core of current carrying energetic electrons. This configuration continued for 40 ms without fatal instabilities.

1 Introduction

A toroidal magnetic system called 'Astron-Spherator' was first considered for plasma confinement by S.Yoshikawa and N.C.Christfilos[1] so as to synthesise the favourable features of Astron [2] and Spherator [3,4]. Spherator is equipped with a conducting hard core carrying toroidal currents. Its magnetic configuration is characterised by deep magnetic well, high magnetic shear and short connection length between the bad and good curvature regions. However, the presence of the hard core, floated and immersed inside the confined plasma, makes it difficult to extend this system to a fusion reactor concept. This drawback would disappear in Astron-Spherator where a relativistic electron beam (REB) ring is used instead of the hard core of Spherator.

In order to preserve attractive characteristics of Spherator in Astron-Spherator, the current carrying REB ring should be concentrated at the central region in the confined plasma so that a wide magnetic region similar to Spherator becomes available. Since this configuration is in a very low q state, the formation of Astron-Spherator might be impossible by using runaway electrons in tokamaks though high current runaway electrons were produced in tokamaks and the shrinkage in their minor radii were suggested[5,6]. In this paper the first experimental evidence is presented of the formation of Astron-Spherator configuration, where the REB ring with a large aspect ratio is surrounded by the confined plasma. This REB ring was formed in a toroidal device SPAC-VI[7] by injecting an intense pulsed REB.

2 Experimental Procedure and Diagnostics

The experiment was carried out with a toroidal device SPAC-VI, the topview of which is schematically shown in Fig.1. An REB ring was formed in a resistive shell, i.e.the vacuum vessel, by injecting a pulsed REB and then the ring was compressed as the external vertical field increased. The principle of this formation was explained in Ref.8 and also the detailed discussion will be made elesewhere[9]. Only a brief description is given here. A pulsed REB (1.3 MeV, 60-150 kA, 80 ns) was injected into a prepared partially ionized hydrogen plasm by using the 'Plasma Anode' method[10] in the presence of both the toroidal and the weak vertical magnetic field. Figure 2 shows the time variations of these fields. An REB ring was formed with the help of the shell effect. Then, the major radius compression proceeded for 2 ms and the compressed ring was held at a nearly constant major radius.

The ring current was measured with a Rogowski coil and the major radius was estimated from the spatial distribution of the poloidal magnetic field which was measured with several magnetic search coils arranged inside the shell. There were also used diagnostic instruments such as an HCN-laser interferometer for the plasma line density, a profile display system[11] of doppler broadenings of impurity line spectra for the ion temperature and a ruby-laser Thomson scattering system for the electron temperature. The Bremsstrahlung emitted in the tangential direction from the ring was detected and analysed in a hard X-ray

region with a time-resolvable X-ray pulse height analyser equipped with a 3"x 3" NaI(Tl) scintillator.

The overall spatial distribution of energetic electrons was inferred by taking photographs with an X-ray pin-hole camera. A pin-hole of 3 mm diameter was bored through a vacuum flange of 1.2 cm thickness at the radius 76 cm from the axis of the device. The hole was vacuum sealed with a Be foil of 25 μm thickness. The space of 6 cm distance between the foil and the film for X-ray photograph was filled with 1 atm He gas to reduce the attenuation of X-rays. The spatially resolvable length is 2 cm at 70 cm from the pin-hole camera. In this experiment, X-ray energy effective to blacken the film(Fuji-X Ray-150) was found to be in the range 2 - 20 keV. The energy lower than 2 keV is cut by the Be foil window, and the upper energy 20 keV was practically found by setting absorbers in front of the film. The relation of the blackening extent to the exposure amount was experimentally found using an isotope ^{55}Fe which emits 5.9 keV X-rays.

3 Experimental Results

Figure 3 shows the time variations of the ring current $I_R(t)$, the line density of electrons n'l and the major radius of the ring current channel R(t) for a typical shot, when an X-ray picture was taken with the pin-hole camera. By the major radius compression with the compression ratio of 2.0, the ring current

increased twice the initial value and the density also became higher. Then, the major radius was kept nearly constant at $R \approx 17\text{-}19$ cm. The doppler temperature of impurity ions slowly decreased after the compression from 80-100 eV to 50 eV in 2 ms, whereas the electron temperature measured 2 ms after the injection was about 10 eV which was nearly the same as the temperature estimated from impurity line intensity ratios in UV light region using the corona equilibrium model.

The X-ray photograph of the ring is shown in Fig.4, together with a schematic drawing indicating the ring position in the vacuum vessel. It is noted that the envelope of the X-ray image is detached far from the inner wall of the vacuum vessel. In Fig.5, there are shown X-ray intensity variations scanned in the horizontal direction on the meridian plane of the torus and those in the vertical direction at three different positions. From the horizontally scanned curve (#-1 in Fig.5(b)) as well as from Fig.4, there exists a clear difference in the emitted X-ray intensity between the forward emission (the left image) and the backward one (the right image). From the vertically scanned curve (#-4 in Fig5(a)) of the left image, the minor radius at the half maximum intensity is estimated to be less than 1.8 cm. The uncertainty of the radius estimation is mainly due to the weak spatial resolution of the pin-hole camera with the aperture of 3 mm diameter, so that the probable true radius is smaller than 1.8 cm. Figure 6 presents the visible light photogragh taken on the same shot. The minor radius of the plasma periphery is about 5 cm which roughly corresponds to the q=1 surface as will be discussed in the next section.

4 Discussion of Experimental Results

The X-ray photograph (Fig.4) and its luminosity-densitometric curves (Fig.5) indicate that the origin of Bremsstrahlung concentrates in a region of the radius a_c less than 1.8 cm on the time average. The power of Bremsstrahlung caused by the interaction of energetic electrons of the density n_b with the plasma is proportional to

$$\sigma n_b \sum_z Z^2 n_z ,$$

where σ is the cross section for Bremsstrahlung and n_z is the density of the ions with atomic number Z. This concentration is due to either the spatial concentration of fairly high Z atoms or the localization of energetic electrons. However, the former situation is improbable in the present experiment, since visible impurity lines were observed in a region wider than the X-ray luminous region. Therefore, it is clear that there exists a core of highly energetic electrons, around which a plasma with the minor radius of about 5 cm is confined, as is seen from the photograph of visible light in Fig.6. Strictly speaking, the core radius a_c is not constant during the life time but the radius decided from the half maximum intensity may give a probable upper bound for the most part of the life time in considering the resolution power of the used pin-hole camera. In Fig.5, the X-ray intensity of the forward Bremsstrahlung is 4 times that of the backward one (Let this intensity ratio be g).

This means that the relativistic electrons are circulating about the torus and their direction is the same to generate the toroidal current observed experimantally.

Figure 7 presents virtual intensitie ratios of the forward Bremsstrahlung to the backward one as a function of a ratio p_p/p_t for different electron energies, where p_p and p_t are the poloidal and the toroidal components of the momenta of thespecified electon. Here, the Born-Approximation [12] is used for the calculation of Bremsstrahlung and the electron is assumed to move on the circle of 17 cm radius with a constant p_p/p_t. For a given intensity ratio, the larger p_p becomes necessary as the electron energy increases. The actual intensity ratio g could be calculated when distributions of the core electrons are well defined in the velocity space as well as in the real space.

The equilibrium condition of the core composed of monoenergetic electrons is rewritten as

$$\left.\begin{aligned} B_v &= \frac{\mu_0}{4\pi R} I_R \left(\ln \frac{8R}{a_c} + \Lambda - \frac{1}{2} \right), \\ \Lambda &= \frac{I_A}{I_R \beta} \left(\beta_t + \frac{\beta_p^2}{2\beta_t} \right) + \frac{\ell_i}{2} - 1, \end{aligned}\right\} \qquad (1)$$

from Ref.13, where B_v is the external vertical field, $I_A = 17000\beta\gamma$ is the Alfven current limit, γ is the relativistic factor of the electron : $\gamma = 1/\sqrt{1 - v^2/c^2}$ (v:velocity, c:light velocity), β_t and β_p are the toroidal and the poloidal components of $\vec{\beta} = \vec{v}/c$, and ℓ_i is the measure of the internal inductance. As the parameters B_v, I_R and a_c are found experimentally, so we can know the electron energy in the assumption of the ratio β_p/β_t and

ℓ_i. In the case 10 ms after the beam injection, where I_R = 43 kA, B_v = 870 G and R = 18 cm, we have $\gamma \approx 1.15$(:75 keV) for ℓ_i = 0.5 and $\beta_t = \beta_p$, $\gamma \approx 1.16$(:84 keV) for β_p = 0. Therefore, the ring current is higher than the Alfvén current limit which is 17~20 kA in this case. Thus, it is the most probable that the core is a current channel, of which the field configuration is nearly in a force-free state where the current exceeds the Alfvén current limit, as has been considered theoretically by S.Yoshikawa[14], J.R.Kan and Hon-Ming Lai[15] and G.Benford[16].

In the case of such a nearly force-free state, the electrons move along the magnetic field lines. Whence we have the relation:

$$\frac{\beta_p}{\beta_t} \approx \frac{B_p}{B_t}, \qquad (2)$$

where B_p and B_t are the poloidal and the toroidal components of the magnetic field. Making use of eq.(2) and assuming a profile of the core current and a monochromatic energy of the electrons, we can numerically estimate the intensity ratio g. Figure 8 shows dependences of the intensity ratio of the monochromatic electron energy for several minor radii of the core in the case of flat current distribution. At the observed intensity ratio g = 4 (see the dotted line), the energy becomes 76 keV for a_c = 1.5 cm or 90 keV for a_c = 1.0 cm. These estimated energies are well in agreement with those deduced from the equilibrium condition. However, the measurement of hard X-rays with the pulse-height analysing system suggested the presence of electrons of energies up to 1.8 MeV. Therefore, it can be concluded that

the energies of the core electrons widely spread but the dominant ones lie near or less than 100 keV.

The magnetic configuration outside the core is numerically examined under the experimental condition. Figure 9 shows the configuration at 5 ms after the beam injection, i.e. at 3 ms after the cease of compression. The core region of 1.5 cm radius is shaded and the numeral noted at each magnetic surface indicates the rotational transform angle ι(= 1/q, q:safty factor) on it. This configuration does not vary appreciably during the time 5 — 15 ms after the beam injection because of the similar decays in both the toroidal field and the ring currents. From the photograph of visible light in Fig.6 and other experimental results such as impurity line images of the ring plasma on a space-resolving spectrometer, it is clear that the plasma edge is located near the rational ι= 1 (i.e.q = 1) magnetic surface inside which ι becomes higher as going to the inner. The magnetic well depth inside the ι = 1 surface is about 15 %. Here, the effect of the plasma current on the configuration is small in this case because the change of the magnetic flux enclosed in the ring could induce only 3 kA at most. Therefore, the plasma is confined in a magnetic configuration generated by the beam core similar to Astron-Spherator.

One of the most important problems in Astron-Spherator is that of gross stability of the current carrying core. Experimentally, the core was stable except the appearance of small stepwise drops in the current. MHD activities observed with magnetic search coils having a frequency resolution up to 10

MHz were so small as $\tilde{B}/B \sim 10^{-4}$ except at the stepwise drops. The wave form of the ring current in a well tuned condition is shown in Fig.10. The current continued for 40 ms which was comparable with the life time of the external magnetic fields. The reason why such an isolated core from the shell is stable is offering further theoretical studies. Here, the model of centrifugal relativistic electron beam[16] may give a suggestion, in which long wavelength modes like the kink are stabilized by applying a weak axial or toroidal magnetic field.

5 Conclusive Remarks

It was experimentally proved that Astron-Spherator configuration is generated by the injection of a relativistic electron beam. In the experiment, a slender ring core of current-carrying energetic electrons produced the poloidal magnetic field and thereby a magnetic configuration with high rotational transform and deep magnetic well was formed. The confined plasma extended to the rational surface of $\iota = 1 (q = 1)$. This outer plama boundary was well detached from the inner surface of the vacuun vessel. In this case poloidal divertors will become very effective for impurity control.

The electron core ring was probably in a nearly force-free state and it continued for 40 ms, comparable with the time duration of the external magnetic fields. The MHD activity was at a very low level except at the appearance of stepwise drops in

the ring current, which were followed with changes in the plasma density.

The energy spread of the core electrons has not been clarified yet and more accurate time-resolved measurement of the core radius is necessary. The reason why such a core is stable is open for further examination.

References

1) S.Yoshikawa and N.C.Christfilos: Plasma Physics and Controlled Nuclear Fusion, 1971 (IAEA, Vienna, 1972) Vol.I, p.357.

2) N.C.Christfilos: Proc. 2nd Int. Conf. on the Peaceful Use of Atomic Energy, Geneva, 1958 (United Nations, Geneva, Switzerland, 1958), Vol.32, p.279.

3) R.Freeman, M.Okayabashi, H.Pacher, G.Pacher and S.Yoshikawa: Phy. Rev. Lett., 23 (1969)756.

4) M.Okayabashi, B.Ripin, J.Schmidt and S.Yoshikawa: Phys. Fluids, 16 (1973)2339.

5) V.S.Vlasenkov, V.M.Leonov, V.G.Merezhkin, V.S.Mukhovatov: Nuclear Fusion, 13 (1973)509.

6) D.A.Spong, J.F.Clark and J.A.Rome: Nuclear Fusion, 13 (1974)397.

7) A.Mohri, K.Narihara, Y.Tomita, T.Tsuzuki, M.Hasegawa and K.Ikuta: Plasma Physics and Controlled Nuclear Fusion Research, 1980 (IAEA, Vienna, 1981) Vol.I, p.511.

8) A.Mohri, K.Narihara, Y.Tomita, M.Hasegawa, T.Tsuzuki and T.Kobata: Phys. Scripta, 25 (1982)509.

9) Y.Tomita, K.Narihara, M.Hasegawa, T.Tsuzuki and A.Mohri: in preparation.

10) A.Mohri, K.Narihara, T.Tsuzuki, Y.Kubota, Y.Tomita, K.Ikuta and M.Masuzaki: Plasma Physics and Controlled Nuclaer Fusion Research, 1978 (IAEA, Vienna, 1979) Vol.III, p.311.

11) A.Mohri, K.Narihara and K.Haba: Res. Rep. of Institute of Plasma Physics, Nagoya Univ., IPPJ-T-34 (1982).

12) H.W.Koch and J.W.Motz: Rev. Mod.Phys., 31 (1959)920.

13) A.Mondelli and E.Ott: Phys. Fluids, 17 (1974)1017.

14) S.Yoshikawa: Phys. Rev. Lett., 20 (1971)295.

15) J.R.Kan and Hon-Ming Lai: Phys. Fluids, 22 (1972)2041.

16) G.Benford: Phys. Fluids, 22 (1979)1527.

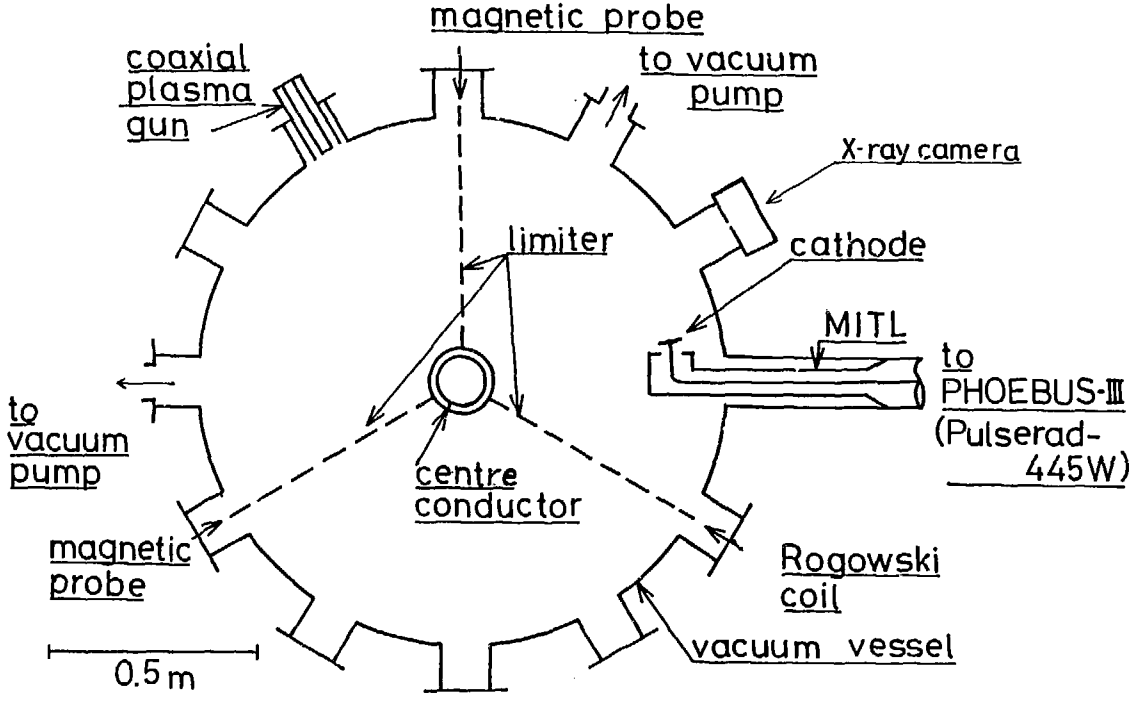

Fig. 1 Schematic top view of a toroidal device SPAC-VI.

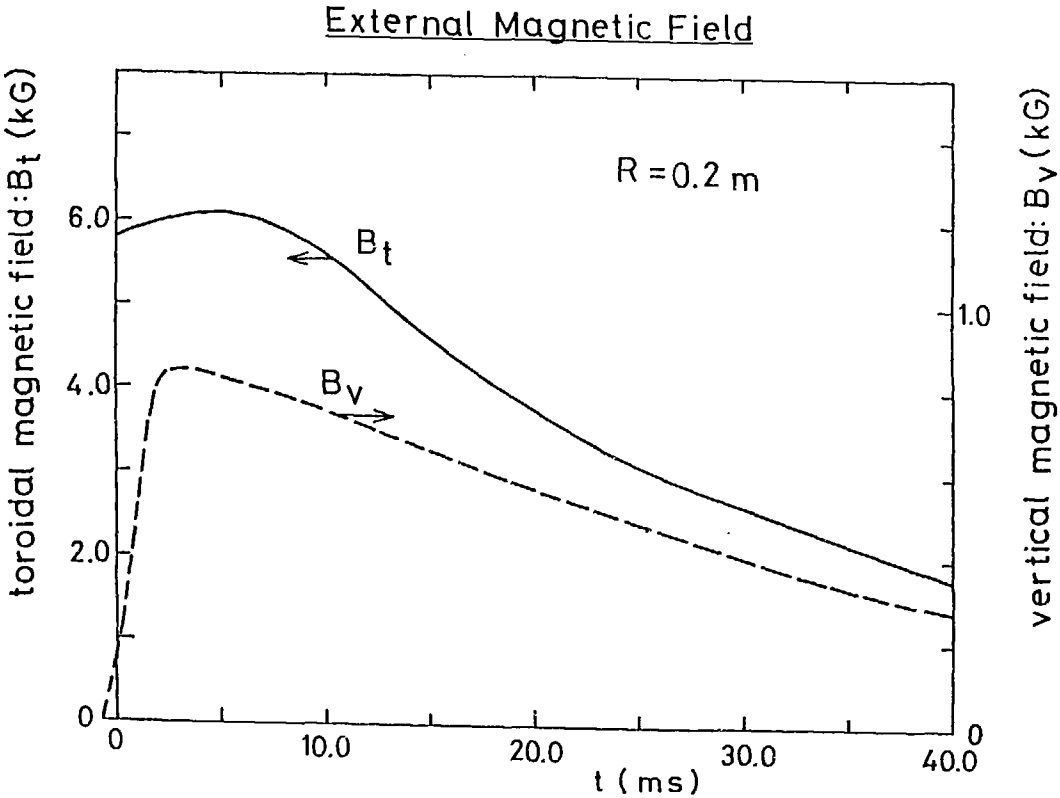

Fig. 2 Time variations of the external toroidal and vertical magnetic fields at the major radius 20 cm.

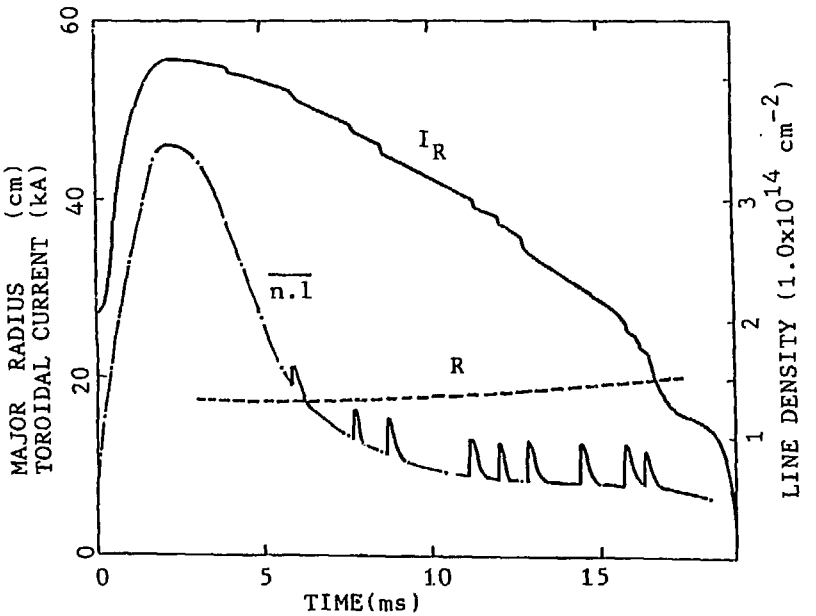

Fig. 3 Time variations of the ring current I_R, the electron line density $\overline{n.l}$ and the major radius of the ring R.

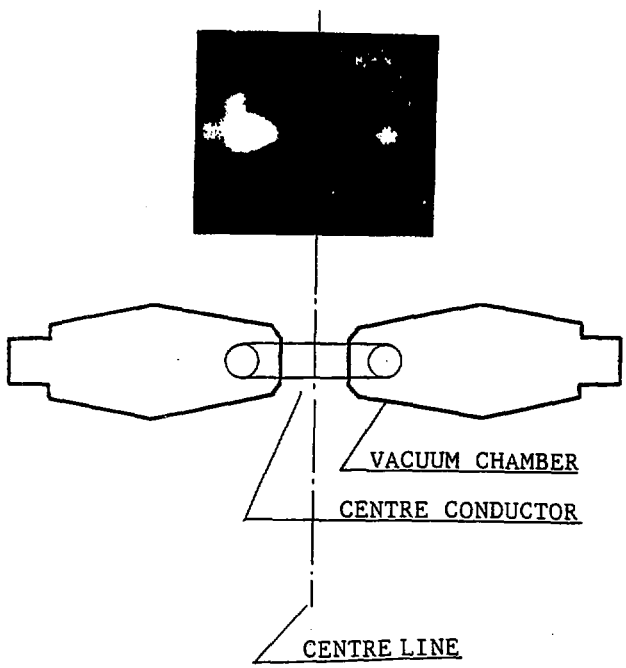

Fig. 4 X-ray photograph of the ring. The left image is due to the forward Bremsstrahlung of circulating electrons and the right is due to the backward one. The ring position in the SPAC-VI vacuum chamber is schematically shown.

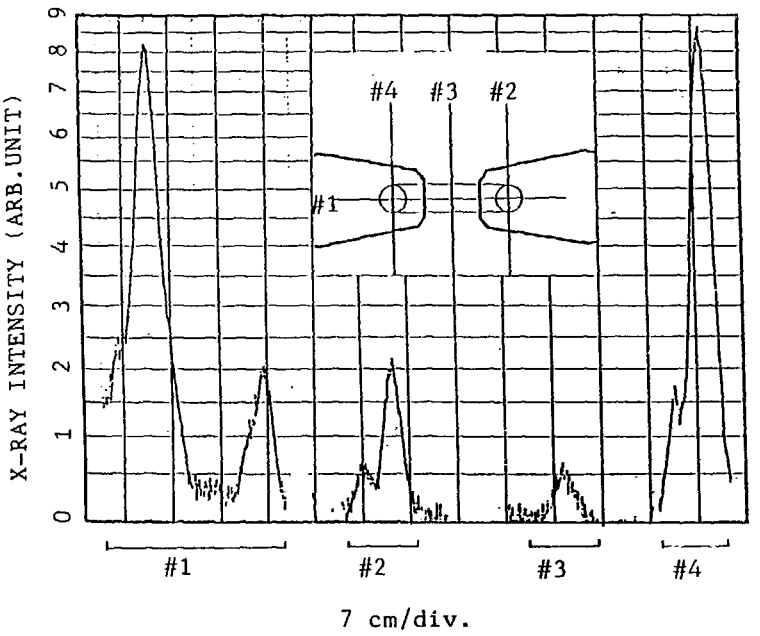

Fig. 5 X-ray intensity variations on different lines shown in the inset.

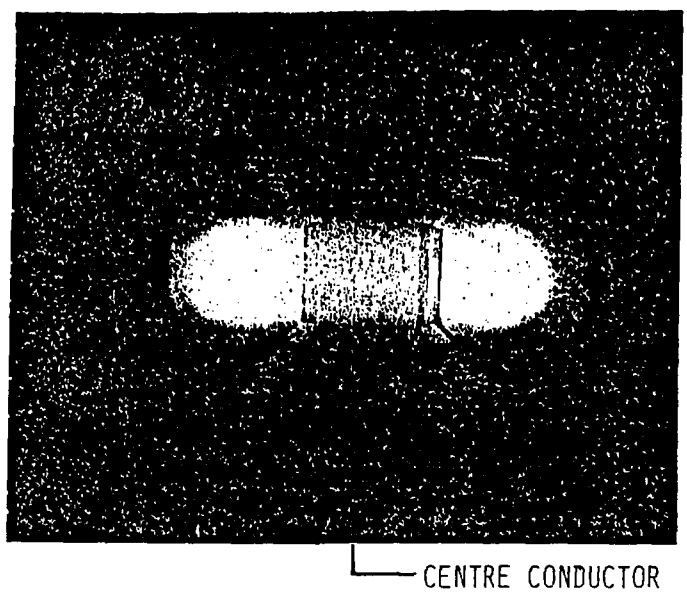

Fig. 6 A visible light photograph of the ring, taken on the same shot as in Fig.4.

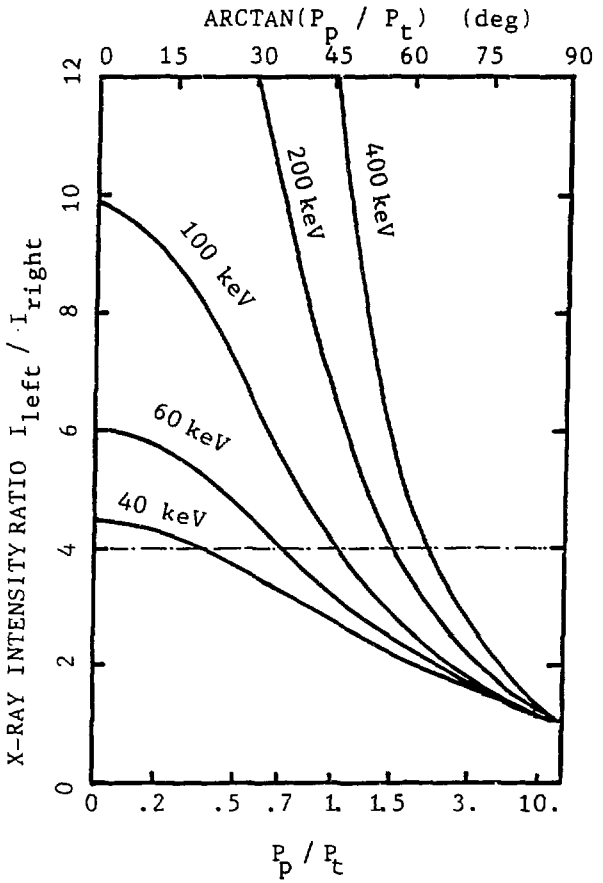

Fig. 7 X-ray intensity ratios I_{left} / I_{right} as a function of the momentum ratio p_p/p_t for various electron energies.

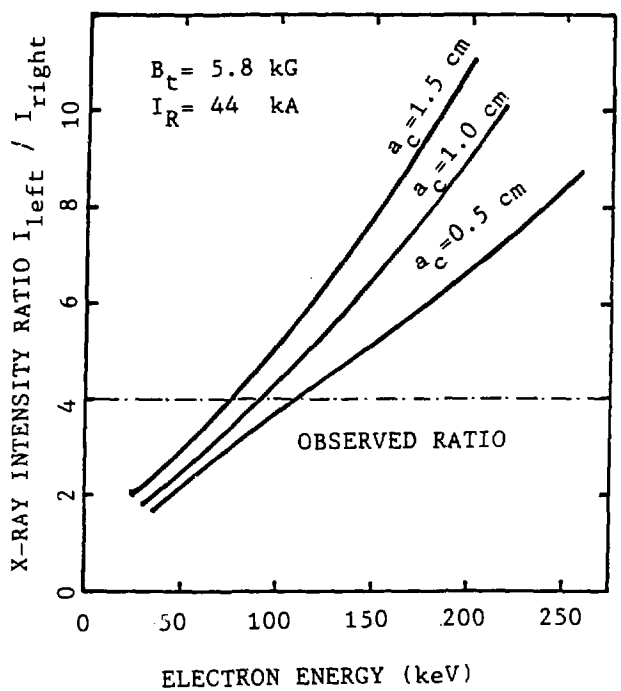

Fig. 8 X-ray intensity ratios I_{left} / I_{right} as a function of electron energy for different minor radii a_c. The electron motion is force-free and the electron current density is uniform in the toroidal direction.

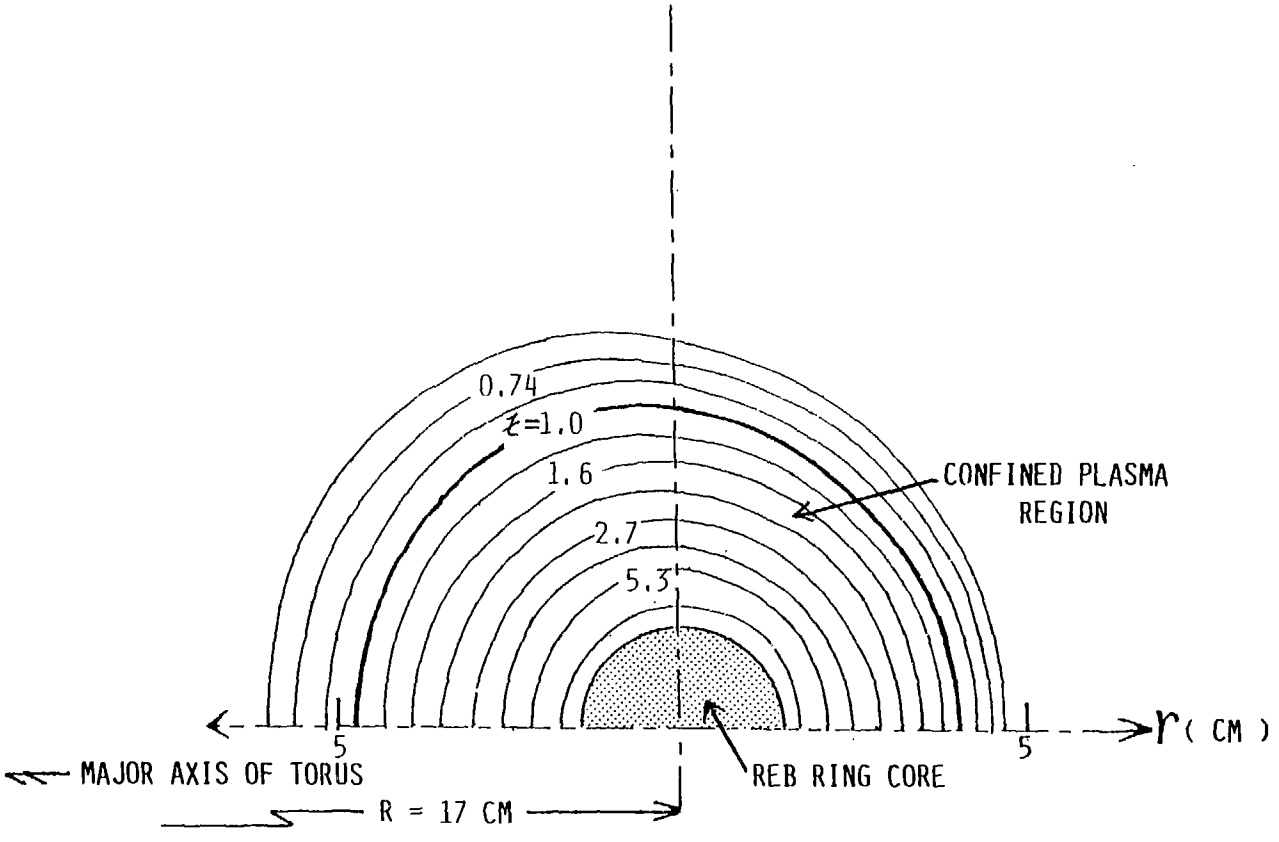

Fig. 9 The magnetic configuration at 5 ms after the beam injection. The numeral noted at each magnetic surface indicates the rotational transform angle ι (= 1/q. q:safety factor). The current core is shown by a dotted area. The magnetic well inside the q = 1 surface is about 15 %.

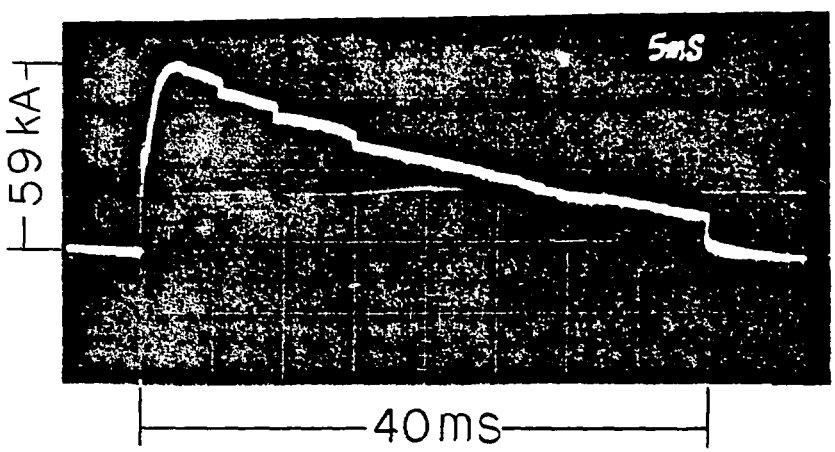

Fig. 10 Oscillogram of the ring current in a well tuned condition.